Effect of Sn doping on the coherent Kondo gap in CeRhSb and the emergence of a non-Fermi-liquid state in $CeRhSb_{1-x}Sn_x$

Andrzej Ślebarski and Tomasz Zawada
Institute of Physics, University of Silesia, ulica Uniwersytecka 4, 40-007 Katowice, Poland

Jozef Spałek
Marian Smoluchowski Institute of Physics, Jagiellonian University, ulica Reymonta 4, 30-059 Kraków, Poland

Andrzej Jezierski
Institute of Molecular Physics, Polish Academy of Sciences, 60-179 Poznań, Poland

(Received 25 March 2004; revised manuscript received 24 June 2004; published 8 December 2004)

CeNiSn and CeRhSb are known as heavy-fermion (Kondo) insulators with a narrow energy gap in the heavy-quasiparticle density of states. The gap appearance is very sensitive to the number of carriers present. Existing studies of alloying show that replacement of Sn ions of CeNiSn by Sb leads to a formation of the weakly ferromagnetic Kondo lattice, whereas CeRhSn has a non-Fermi-liquid ground state. In view of the contrasting behavior of the Sb-containing and Sn-containing systems, we investigate the solid solutions $CeRhSb_{1-x}Sn_x$, to determine the dependence of the electronic properties on the number of the conduction electrons and, in particular, on the gap formation in CeRhSb, as well as on the nature of the ground state across the series. We present the structural properties, the electronic band structure, and the resistivity $[\rho(T)]$ data for $CeRhSb_{1-x}Sn_x$. The system exhibits in the Sb-rich regime a variety of $\rho(T)$ dependencies at the low temperatures, namely, an activated behavior $\rho=\rho_0 \exp(\Delta_{coh}/k_BT)$ for $x=0$ and $x=0.1$, $\rho \propto T^2$ for $x=0.2$, which transform into the dependences $\rho \propto -\ln T$ for $x=0.9$, and $\rho \propto T^{\epsilon}$ (where $\epsilon \sim 1$) for Sn-rich samples. Furthermore, the resistivity of both the CeRhSb and the Sn-substituted alloys indicates a coherent Anderson-lattice nature of the ground state. We also present the $3d$ x-ray photoemission (XPS) spectra, from which we determine the f-shell occupation. Analysis of the $3d^9f^2$ weight in the $3d$ XPS spectra, using the Gunnarsson-Schönhammer model, suggests that the hybridization Δ_{fs} is about 150 meV across the $CeRhSb_{1-x}Sn_x$ series. The XPS valence band spectra (high-energy probe) for $CeRhSb_{1-x}Sn_x$ are related to the linear muffin tin orbital calculations. We interpret the XPS data in terms of the band-structure calculations, whereas the $\rho(T)$ and the magnetic susceptibility $\chi(T)$ data (low-energy probes) in terms of Anderson-lattice physics.

DOI: 10.1103/PhysRevB.70.235112 PACS number(s): 71.27.+a, 71.28.+d, 75.40.Cx, 73.20.At

I. INTRODUCTION

Cerium-based Kondo- (Anderson-) lattice systems exhibit unusual physical phenomena such as heavy-Fermi-(HF) liquid or non-Fermi-liquid types of behavior in a metallic state or a Kondo-lattice insulating type of state. Typical examples of such cerium-containing Kondo insulators with a very narrow energy gap in the electronic density of states (DOS) are CeNiSn (Ref. 1) and CeRhSb.[2] The nonmagnetic insulating state of both compounds settles down at low temperature, but they become HF metals at higher temperature $T>T_K$, when the gap disappears.[3] The first qualitative picture of both HF metals and Kondo insulators was based on the idea that the ground-state results from a competitive character of the Kondo and the Ruderman-Kittel-Kasuya-Yosida (RKKY) interactions.[4] If the RKKY interaction predominates, various magnetic ground states can occur with an antiferromagnetic order appearing at temperature T_N. If the Kondo interaction predominates, the hybridization between the localized f-electron and the $5d$-$6s$ conduction states can lead to a formation of either a coherent heavy-Fermi liquid or to a gap/pseudogap formation at the Fermi energy when temperature $T\rightarrow 0$ (see, e.g., Ref. 5). A refined picture is based on the Anderson-lattice model and the formation of very narrow band states of width k_BT_K, which plays both the role of the coherence temperature for heavy quasiparticle states, as well as characterizes the hybridization gap in case of the Kondo insulators.[6]

A paramagnetic Kondo insulator discussed within the periodic Anderson model provides an insulating state for a k-independent hybridization and for an even number of strongly correlated electrons per unit cell.[7] Additionally, the numerical calculations show that the Kondo gap depends strongly on the magnitude of hybridization between Ce $4f$ and the transition metal d states,[8] since the Ce $4f$ and Sn or Sb $5p$ mixing is small. In the case of the momentum-dependent hybridization ($V_{\mathbf{k}}$), the gap may vanish at either some points or along the lines where $V_{\mathbf{k}}=0$, providing thus a semimetallic ground state of the system.

The stability of paramagnetic vs magnetic ground state in the Kondo-lattice limit[9] is also strongly dependent on the number of electrons per atom. Therefore, the energy gap in Ce-based Kondo insulators is very sensitive to the partial heteroelectronic substitution.[10–12] Previous alloying studies showed that substituting either Sb ions for Sn in CeNiSn (Ref. 13) or Sn ions for Sb in CeRhSb (Ref. 14) leads either to a formation of weak ferromagnetic Kondo lattice or to the non-Fermi-liquid ground states, respectively.

TABLE I. Crystallographic and transport characteristics of the $CeRhSb_{1-x}Sn_x$ series as a function of x.

x	structure	lattice parameters in Å a	b	c	T_{max} (K)	T_{min} (K)	$\rho(T)$ dependence
0	ϵ−TiNiSi	7.417	4.622	7.866	130	285	$\rho=\rho_0\exp(\Delta_{coh}/k_BT)$ for $T<6$ K
0.1	ϵ−TiNiSi	7.409	4.615	7.846	102	325	$\rho=\rho_0\exp(\Delta_{coh}/k_BT)$ for $T<7$ K
0.2	ϵ−TiNiSi	7.406	4.619	7.852	73	305	$\rho=\rho_0+aT^2$ for $T<20$ K
0.8	Fe_2P	7.460		4.068	44	300	critical behavior at $T_0=7.8$ K
0.9	Fe_2P	7.461		4.078	56	236	$\rho\propto-\ln T$ for $T<16$ K
0.95	Fe_2P	7.478		4.096	60	300	$\rho=\rho_0+aT^{0.5}$ for $T<25$ K
1	Fe_2P	7.444		4.081	100	240	$\rho=\rho_0+aT^{0.92}$ for $T<25$ K

The compound CeRhSn exhibits a non-Fermi-liquid character of the temperature dependence for low-temperature physical properties,[14] which were discussed in terms of the Griffiths phase model.[15,16] It has been shown that the electrical resistivity change rises as a function of temperature according to $\Delta\rho\sim T^{\epsilon}$, with the exponent $\epsilon\cong 1$, whereas both the quantity C_p/T related to the specific heat C_p, as well as the magnetic susceptibility χ, vary as T^{-n}, with $n\cong 0.5$.[14]

In view of the diverse behavior of CeRhSb with respect to that of CeRhSn, it is of interest to examine the solid solution $CeRhSb_{1-x}Sn_x$, to see the effect of the decreasing number of conduction electrons (with the increasing x) on the gap formation in CeRhSb, as well as to trace the changes in the ground state properties across the series. It is also important to see how a coherent Kondo-lattice state evolves with the increased substitution of Sn. Our measurements indicate that the gap in CeRhSb is rapidly suppressed even by a small amount of Sn, though the XPS spectra continue to show a mixed-valent behavior of the Ce ions. Furthermore, the NFL behavior in CeRhSn is suppressed even by a small Sb substitution.

The aim of this work is to investigate the electronic structure, the crystallographic properties, the electrical resistivity, and the static magnetic susceptibility of $CeRhSb_{1-x}Sn_x$. We also compare the valence-band XPS spectra with the electronic-structure calculations for the valence bands. The first part represents a discussion of the systems $CeRhSb_{1-x}Sn_x$ by a high-energy probe and is followed by its characterization in terms of an overall single-particle electronic structure. In the second part we supplement the analysis with the discussion of temperature dependence of the resistivity and the static susceptibility, that allows for a characterization of the system in terms of the temperature dependence of the coherent Kondo gap or of a non-Fermi-liquid behavior, depending on the system composition.

II. EXPERIMENTAL DETAILS

Polycrystalline samples of $CeRhSb_{1-x}Sn_x$ have been prepared by arc melting of the constituent elements on a water cooled copper hearth in a high purity argon atmosphere with a Zr getter. Each sample was remelted several times to improve its homogenity and annealed subsequently at 800 °C for 2 weeks. The samples were carefully examined by x-ray diffraction analysis and found to be single phase for $x<0.2$ (orthorhombic ϵ-TiNiSi structure, space group *Pnma*) and for $x\geqslant 0.8$ (hexagonal of the Fe_2P type, space group $P62m$).

The x-ray diffraction studies also showed, however, that for $0.2<x<0.8$ the samples were not single-phase materials and consisted of CeRhSb and CeRhSn. The lattice parameters provided in Table I were acquired from the diffraction patterns analysis using the POWDER-CELL program.

Electrical resistivity measurements were made using a standard four-wire technique. The x-ray photoelectron spectroscopy (XPS) spectra were obtained with monochromatized A1 K_α radiation at room temperature using a PHI 5700 ESCA spectrometer. The spectra were measured immediately after cleaving the sample in a vacuum of 10^{-10} Torr. The spectra were calibrated according to a prescription described in Ref. 17. Binding energies were referenced to the Fermi level ($\epsilon_F=0$).

The electronic structure of the ordered compounds was studied by the all-electron self-consistent linearized muffin-tin orbital (LMTO) method and the calculations were performed using the tight-binding (TB) LMTO-4.7 code.[18] In the approximate (TB-LMTO) method the crystal potential is treated within the atomic sphere shape approximation (ASA)[19] with overlapping Wigner-Seitz (WS) spheres centered at atomic positions. The values of the WS sphere radii were determined in such a way that the sum of all atomic sphere volumes is equal to the volume of the unit cell. The electronic structures were computed for the experimental lattice parameters listed in Table I. In both methods the local spin density approximation (LSDA) for the exchange correlation (XC) potential was employed. In the TB-LMTO calculations the XC potential was assumed to be of the form proposed by von Barth-Hedin,[20] and Langreth-Mehl-Hu (LMH) generalized gradient corrections were included.[21] The randomly diluted system, say $CeRhSb_{0.1}Sn_{0.9}$, is regarded as an effective periodic medium with one atom of Sn in ten replaced by the Sb atoms.

III. HIGH-ENERGY PROBES

A. Electronic band structure

It has been controversial whether the ground state of CeNiSn or CeRhSb is in a semiconducting or in a semimetallic state with a very low carrier density of states (DOS) or with a V-shape pseudogap. Different experiments (NMR,[22]

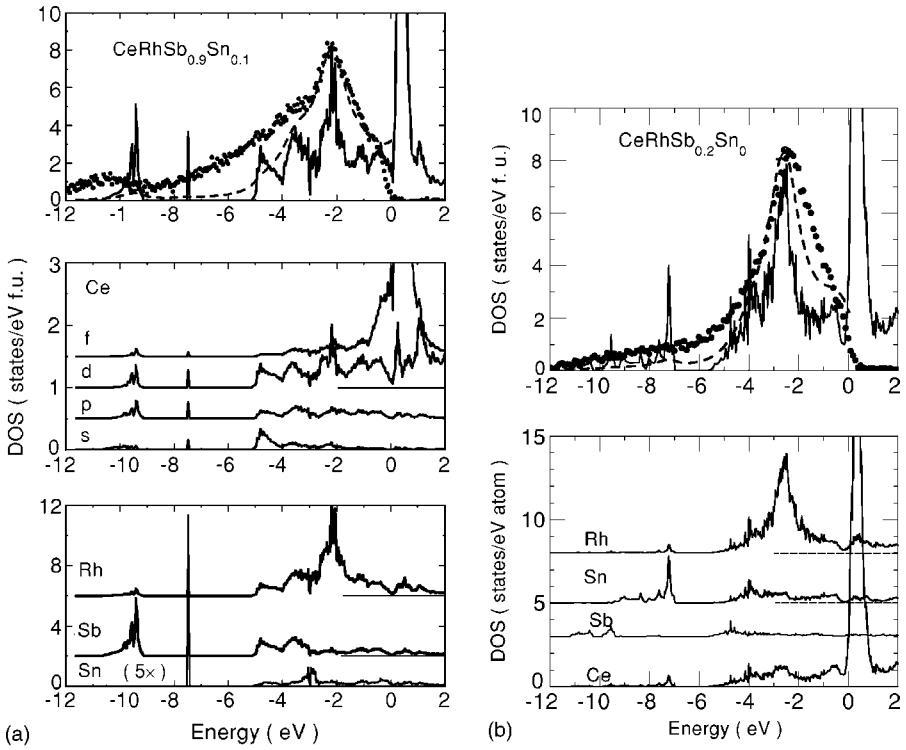

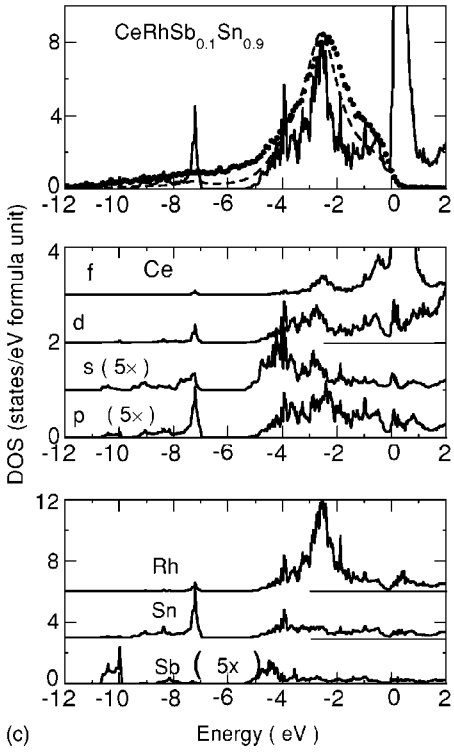

FIG. 1. Comparison of the total DOS calculated for $CeRhSb_{0.9}Sn_{0.1}$ (a), $CeRhSb_{0.2}Sn_{0.8}$ (b), and $CeRhSb_{0.1}Sn_{0.9}$ (c); convoluted with Lorentzians of half-width 0.4 eV, taking into account proper cross sections for bands with different l symmetry (thick curve), and the measured XPS valence bands corrected by the background (points). The partial DOS curves are ploted below.

specific heat,[23] ultrahigh-resolution photoemission spectroscopy[24]) have shown the appearance of a residual density of states within the energy gap. Electronic band structure calculations also predict the small DOS at c_F for either CeNiSn (Ref. 25) or CeRhSb (Ref. 26). Obviously, the presence of a small Kondo gap in these pure compounds cannot be characterized reliably within the band approach, as discussed in the part B below.

In Figs. 1(a)–1(c), we present numerical calculations of the electronic density of states of $CeRhSb_{1-x}Sn_x$ for $x=0.1$, 0.8, and 0.9. Also shown in the figures, for comparison, are the XPS valence band (VB) spectra. The DOS were convoluted with the Lorentzians of half-width 0.4 eV, to account for the instrumental resolution. The total DOS were multiplied by the corresponding cross sections.[27] A background, calculated by means of a Tougaard algorithm,[28] was subtracted from the XPS data. The overall agreement between the calculated and the measured XPS VB spectra is good.

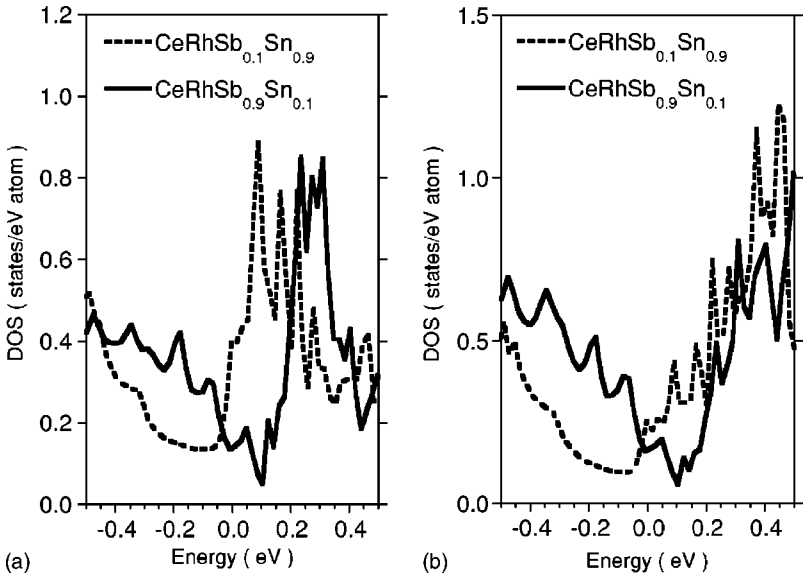

FIG. 2. Comparison of (a) Ce *d* and Rh *d* (b) DOS calculated for $CeRhSb_{0.9}Sn_{0.1}$ and $CeRhSb_{0.1}Sn_{0.9}$ near the Fermi level.

For the compounds of the series $CeRhSb_{1-x}Sn_x$ with $x-0.9$ and 0.8 the total DOS spectra decomposes into two clearly separated parts. A band located in the binding energy (BE) range of 7–11 eV and separated by a gap of ~2 eV from the valence band originates mainly from the *s* states of Sb and Sn [Figs. 1(a) and 1(b)]. For $CeRhSb_{0.9}Sn_{0.1}$ these *s* states of Sb and Sn are separated by a gap of ~2 eV [Fig. 1(c)]. The part of the valence band which extends from 5 eV to ϵ_F is composed mainly of Rh 4*d* states. The Ce 4*f* states become dominant of the total DOS around the Fermi level (Fig. 1), while the distribution of the Ce *d* states as well as Rh *d* states in the narrow vicinity of ϵ_F are radically different for samples of the series $CeRhSb_{1-x}Sn_x$ with $x=0.1$ and $x=0.9$.

In Fig. 2(a) comparison of Rh *d* [Fig. 2(a)] and Ce *d* [Fig. 2(b)] contributions to the DOS is shown for $CeRhSb_{0.9}Sn_{0.1}$ and $CeRhSb_{0.1}Sn_{0.9}$. The DOS presented in Fig. 2 signals a local minimum (i.e., a pseudogap) at ϵ_F in the *d* bands of $CeRhSb_{0.9}Sn_{0.1}$ while the DOS signals a local maximum in the *d* bands of $CeRhSb_{0.1}Sn_{0.9}$. Considering the fractional valence of Ce in CeRhSn and its hybridization energy V between the *f*- and conduction-electron states, which is compared with that of the Ce-Kondo insulator, we try to explain the reasons which could remove a hybridization gap in CeRhSb when Sb is substituted by Sn. First, the spacing between Ce atoms in CeRhSn $d_{\text{Ce-Ce}} \cong 0.39$ nm (Ref. 14) is very close to the Hill limit.[29] Therefore, one expects *f* electrons to be more localized in CeRhSn than in CeRhSb. However, this pseudogap represents a precursory effect rather than a Kondo gap, as the band calculations do not include *f*-electron correlations.[30]

B. Ce 3*d* XPS spectra

The XPS spectra of the 3*d* core levels provide an more detailed information about the 4*f* shell configurations and the *f*-conduction-electron hybridization. The Ce-intermetallic compounds often show different final states depending on the occupation of the *f* shell: f^0, f^1, and f^2 (see Refs. 31 and 32). Figure 3(a) shows the Ce 3*d* XPS spectra obtained for the series of compounds $CeRhSb_{1-x}Sn_x$. Three final-state contributions f^1 and f^2 are clearly observed, which exhibit a spin-orbit splitting $\Delta_{SO} \cong 18.6$ eV. The presence of the f^0 component in the 3*d* XPS spectrum of CeRhSb and CeRhSn, marks clearly the intermediate valence character of Ce atoms.[31,32] Gunnarsson and Schönhammer (GS) explained in Ref. 31 how to determine the initial *f*-state properties from the Ce 3*d* XPS spectra, which are related to the final *f* states. In particular, they discussed how experimental spectra can be used to estimate the *f* occupancy n_f and the hybridization energy Δ_{fs} between the *f*-level and the conduction states. The f^2 components in the Ce 3*d* XPS spectra in Fig. 3(a) are attributed within the Gunnarsson-Schönhammer model to the *f*-conduction electron hybridization. The hybridization energy Δ_{fs}, which describes the hybridization part of the Anderson impurity Hamiltonian,[33] is defined as $\pi V^2 \rho_{\max}$, where $\rho_{\max}$ is the maximum in the DOS and V is the hybridization matrix element. It is possible to estimate Δ_{fs} from the ratio $r=I(f^2)/[I(f^1)+I(f^2)]$, calculated as a function of Δ_{fs} in Ref. 32, when the peaks of the Ce 3*d* XPS spectra that overlap in Fig. 3 are separated. At 885 eV there is also an overlap of the $3d_{5/2}f^1$ final states with the Sn 3*s* peak. The separation of the overlapping peaks in the Ce 3*d* XPS spectra was made using the Doniach-Šunjić approach.[34] The intensity ratio gives for CeRhSb and CeRhSn a crude estimate of a hybridization width ~150 meV. For the $CeRhSb_{1-x}Sn_x$ compounds the hybridization energy is similar.

In order to determine the ground state *f* occupation from the 3*d* XPS spectra we use Fig. 4 of Ref. 32, where the dependence of the ratio $I(f^0)/[I(f^0)+I(f^1)+I(f^2)]$ on the *f* occupation is shown for $\Delta=120$ meV. Relative f^0 intensities of magnitude ~0.07 for CeRhSn, ~0.1 for CeRhSb, and ~0.05 for the remaining $CeRhSb_{1-x}Sn_x$ compounds correspond to the n_f values of the order 0.87, 0.83, and 0.89, respectively.[35] The Ce 3*d* XPS spectra, however, allow an estimate of the occupation number n_f, and of the energy Δ within the accuracy of the order of 15%. The errors are due to the uncertainties in the intensity ratios, which can be attributed to the uncertainty of the spectra decomposition[36], the

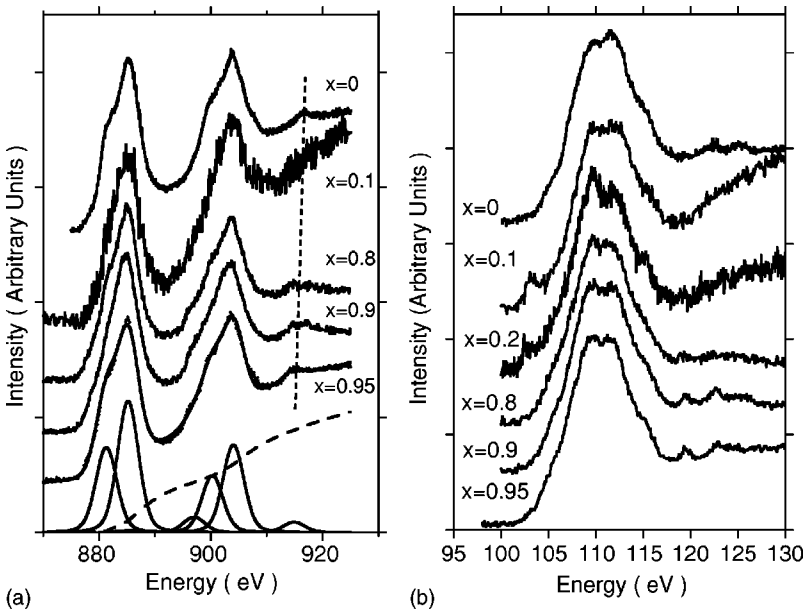

FIG. 3. Ce 3*d* XPS spectra (a) and Ce 4d XPS spectra (b) obtained for $CeRhSb_{1-x}Sn_x$. The f^0, f^1, and f^2 components [(in (a)] are separated on the basis of the Doniach-Šunjić theory. The Sn 3*s* peak at 885 eV provides ~2% of the total peak intensity due to the $3d_{5/2}4f^1$ final states. The dotted line in the inset (a) shows an energetic position of the peak $3d_{3/2}4f^0$ in the Ce 3*d* XPS spectra.

background subtraction, and the surface-to-bulk ratio,[37–39] as well as to the approximations in the GS theory. Moreover, according to GS, the deviation from the linearity of the intensity ratio of the final- to the ground-state *f*-occupation number depends on Δ, which is also obtained within the same accuracy. We, however, conclude that the coupling Δ is strong for CeRhSb, CeRhSn, and $CeRhSb_{1-x}Sn_x$ alloys; in consequence, the Ce atoms are in the mixed-valent state. The Kondo resonance in such a mixed-valent system then forms the two peaks and hence (at $T=0$) a gap/pseudogap can be formed in the electronic density of states; this is the case of CeRhSb, as we shall see in detail from the low-energy measurements.

There is another evidence for an fluctuating valence of Ce ion in $CeRhSb_{1-x}Sn_x$, as shown in Fig. 3(b). The Ce 4*d* XPS spectra exhibit two peaks above 120 eV which can be assigned to the f^0 final state.[40,41,32] In Fig. 3(b), the indicated splitting $\delta=3.1$ eV has almost the same value as the spin-orbit splitting of the La 4*d* states.

C. Bare versus renormalized electronic structure

So far, we have interpreted our XPS spectra in terms of LMTO band structure, which obviously does not take into account the high *f-f* electronic correlations present in the thermodynamic behavior. Therefore, this interpretation may serve only as a qualitative characterization at best and does reproduce the main features of the observed spectra. In the next section we discuss the effect of strong *f-f* correlations on the low-energy properties such as the zero-field magnetic susceptibility and the static electrical conductivity.

IV. LOW-ENERGY PROBES

A. Electrical resistivity and static magnetic susceptibility

In the preceding section we have discussed the electronic structure on an eV (high-energy) scale. Those studies, as we have seen, provide only a qualitative characterization of the bare hybridization magnitude as characterized by the virtual bound-state width Δ_{fs}. Below we concentrate on the low-energy probes, namely, on the electrical resistivity and the static magnetic susceptibility. This should provide a direct estimate of the Kondo coherence gap Δ_{coh}.

In Fig. 4 we display the electrical resistivity ρ versus temperature T for the series $CeRhSb_{1-x}Sn_x$. The resistivity curve has a maximum at the temperature T_{max} followed by a minimum at T_{min}. The values of T_{max} and T_{min} are tabulated in Table I. These results will be discussed in detail below.

To see the onset of the Kondo-lattice gap formation for the Sb rich systems, we have plotted in Figs. 5(a) and 5(b) both the magnetic susceptibility and the resistivity. Both the resistivity and the magnetic susceptibility of CeRhSb are typical for cerium valence-fluctuation compounds having a nonmagnetic ground state. The ionic two-interconfigurational-fluctuation (ICF) model proposed by Sales and Wohlleben[42] determines how much of the suscep-

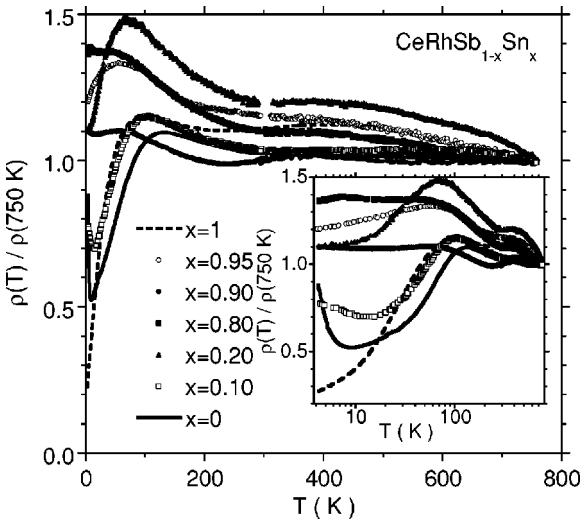

FIG. 4. Electrical resistivity $\rho(T)/\rho(750\ \mathrm{K})$ versus T of $CeRhSb_{1-x}Sn_x$. Also are shown $\rho(T)/\rho(750\ \mathrm{K})$ versus $\ln T$ (inset).

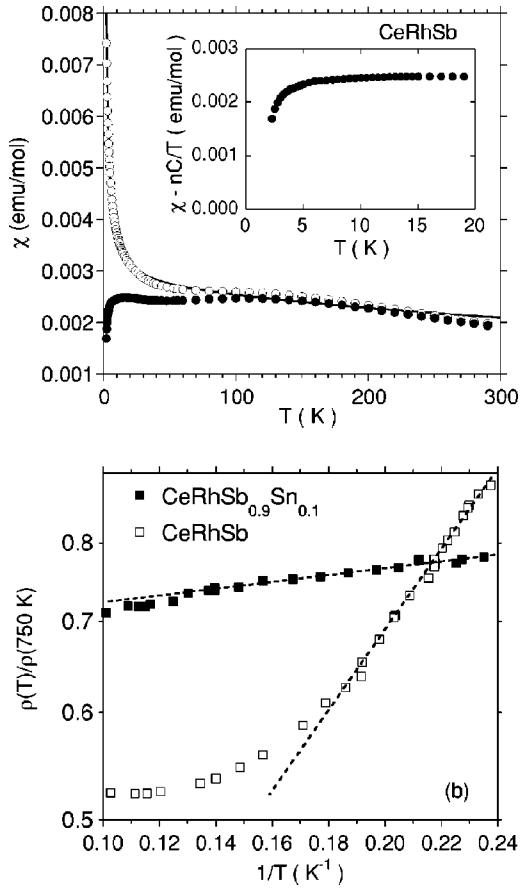

FIG. 5. (a) Magnetic susceptibility χ for CeRhSb (open points) and the χ data subtracted with Curie term nC/T causes by a fraction n of paramagnetic Ce impurities ($n=0.016$). The solid line is a fit based on the ICF model. Inset shows the susceptibility $\chi_f \equiv \chi - nC/T$ as a function of T for $T<20$ K. (b) Reduced resistivity $\rho(T)/\rho(750\ \mathrm{K})$ on a logarithmic scale versus $1/T$ for CeRhSb and $CeRhSb_{0.9}Sn_{0.1}$.

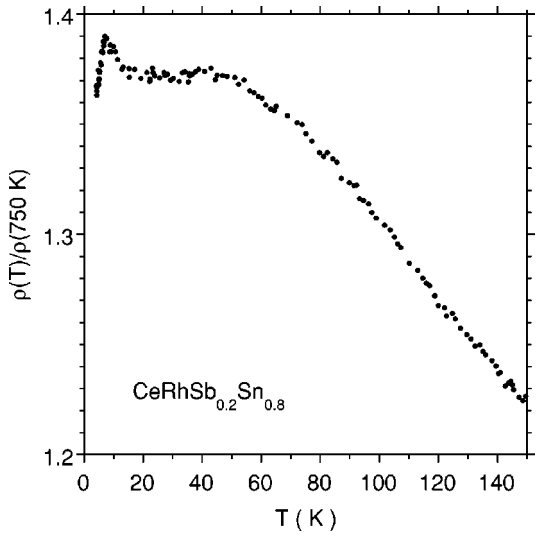

FIG. 6. Electrical resistivity $\rho(T)/\rho(750\ \mathrm{K})$ for $CeRhSb_{0.2}Sn_{0.8}$ versus temperature. Maximum of a sharp peak in $\rho(T)$ which is attributed to a critical behavior, which is located at $T=7.8$ K. The exact nature of this behavior is not determined.

tibility reported in Fig. 5(a) is intrinsic. The solid line represents $\chi(T)=\chi_0+nC/T+n_f^{\chi}\chi_{4f^1}(T^*)$, where $T^*=T+T_{sf}$ fit based on this model with parameters: $\chi_0=7.4\times10^{-4}$ emu/mol, $n=1.6\times10^{-2}$, $T_{sf}=250$ K, and $n_f^{\chi}=0.71$. The occupation number n_f^{χ} is slightly smaller than the n_f value obtained from the XPS spectra. However, what is the most striking feature of the subtracted data is their abrupt decrease for $T<T_K$, as it should be for the Kondo insulators. Additionally, in Fig. 5(a) we have singled out the magnetic impurity part (nC/T); the remaining part (the lower curve, full points) dives down below the temperature $T_K\cong6.5$ K, as seen from the inset to the figure. The strong reduction of the part $\chi_f\equiv\chi-nC/T$ below 6.5 K is in agreement with the notion that the Kondo insulator represents a filled band of heavy quasiparticles. The value of the susceptibility χ_f is flat above T_K and represents a strongly enhanced value $\sim2.5\times10^{-3}$ emu/mol, i.e., in the range for HF systems. Also, the $\rho(T)$ data presented in Fig. 5(b) are typical for a nondegenerate semiconductor with the interband activation energy 6.6 and 0.5 K for CeRhSb and $CeRhSb_{0.9}Sn_{0.1}$, respectively. Again, the gap disappears at approximately the same value of T. So, both $\chi(T)$ and $\rho(T)$ data are consistent with the appearance of the Kondo gap in the spectrum at temperature $T_K\cong6.5$ K.

To single out the transformation from the Kondo insulator/heavy Fermi metal to a non-Fermi liquid, we have displayed in Fig. 6 the $\rho(T)$ dependence for the sample with $x=0.8$. We observe a rather sharp feature around $T_0=7.8$ K on the background of a typical wide maximum. Below we speculate that the narrow $\rho(T)$ peak may be attributed to the quantum critical properties of the NFL instability, which may appear at a nearby concentration.

B. Physical discussion

The temperature $T_{\max}$ characterizes experimentally the resistivity drop $\rho(T)$ upon cooling. The Kondo lattices are usually discussed in terms of the two temperature scales: the usual single-impurity Kondo scale and the coherence. The first is responsible for $T_{\min}$ and the latter is reflected in $T_{\max}(<T_{\min})$ in the $\rho(T)$ curves. At T_K, the usual minimum, followed by a rise in the resistivity, is observed with the decreasing T until at $T_{\max}$ the resistivity shows a drop with the decreasing temperature (see Fig. 4). This drop results from a formation of a coherent Kondo lattice. Thus, at low temperature in the Kondo lattice system there is a competition between a tendency for the resistivity to increase due to the Kondo effect and to its decrease because of the singlet nature of the coherent ground state (e.g., see the discussion of $CeAl_3$ in Ref. 43). Theoretically, the quantum coherence (i.e., the appearance of heavy quasiparticle states) is associated with the effective Kondo (hybridization) temperature T_K, not with the temperature $T_{\max}$, which represents a good characteristic from the experimental point of view. The low-lying excitations in the Anderson- (Kondo-) lattice state appear below $T_K<T_{\max}$, which is

$$T_K = \frac{W}{2}\exp\left(-\frac{1}{J_K\rho^0}\right), \tag{1}$$

where W is the bandwidth of the bare band ($5d$-$6s$) states with DOS at the Fermi level equal to ρ^0. The value J_K is the usual Schrieffer-Wolff exchange coupling integral[44]

$$J_K = 2V^2\left(\frac{1}{\epsilon_f} + \frac{1}{\epsilon_f + U}\right), \tag{2}$$

where ϵ_f is the bare $4f$ level location with respect to the Fermi level and U is the magnitude of the intraatomic (f-f) Coulomb repulsion between electrons. Strictly speaking, the value (1) of T_K, apart from having the sense of the Kondo temperature, depends, in the lattice case, explicitly on the temperature. Namely, for $T \ll T_K$ we can write

$$T_K(T) = T_K + \frac{\pi^2}{6}T_K\left(\frac{T}{T_K}\right)^2 + o\left[\left(\frac{T}{T_K}\right)^4\right]. \tag{3}$$

The principal importance of the function T_K in the Anderson-lattice case is connected with the circumstance that it characterizes both the width of the lowest hybridized states, as well as the value of the Kondo gap ($\Delta_K = 2k_BT_K$) in the low-temperature range. In the regime $T \ll T_K$ the contribution to the specific heat of the type $C_v \sim T^{-1/2}\exp(-T_K/T)$. Also, both the resistivity and the susceptibility should exhibit the activated type of behavior.

Let us now apply these above mean-field results to the discussion of the experimental data. The systems $CeRhSb_{1-x}Sn_x$, as is clearly seen from Table I, exhibit a variety of $\rho(T)$ dependences at $T \ll T_{\max}$.

(i) The systems CeRhSb and $CeRhSb_{0.9}Sn_{0.1}$ exhibit the activated behavior [(See. Fig. 5(a)] $\rho = \rho_0\exp(T_K/T)$, with $T_K \cong 6.6$ K for the stoichiometric material and $T_K \cong 0.5$ K for $CeRhSb_{0.9}Sn_{0.1}$.

(ii) $\rho(T)$ data for CeRhSn and $CeRhSb_{0.05}Sn_{0.95}$ show a non-Fermi-liquid behavior $\rho(T) \sim T^{\epsilon}$, with $\epsilon = 0.92$ and 0.5, respectively.

(iii) $\rho(T) \propto T^2$ for $CeRhSb_{0.8}Sn_{0.2}$, characteristic of the Fermi liquid, whereas $\rho \propto -\ln T$ for $CeRhSb_{0.9}Sn_{0.1}$.

(iv) a singular behavior for $x = 0.8$ sample, indicative of a critical behavior before NFL metallic state sets in.

The result (iii) means that the NFL state transforms gradually into the Fermi-liquid state, which eventually becomes a Kondo insulator upon further adding of electrons to the system, i.e., filling the lower hybridized band of heavy quasiparticles. In the complementary regime $x \geqslant 0.8$ we observe an evolution into the NFL state. The sample with $x = 0.8$ requires further investigations of a possible presence of the critical behavior for $T \cong 7.8$ K. Unfortunately, we have been unable to synthesize the samples in the concentration range $0.2 < x < 0.8$. Nonetheless, the existing samples, when examined further, should substantiate quantitatively the behavior listed as (i)–(iv).

It is amazing that neither the polycrystalline nature nor the atomic disorder destroy, upon substitution, this subtle quantum coherence effects of the $4f$ states, achieved on the scale of 10 K or even less. This implies, that since these systems possess a large number of valence electrons per formula (18 for CeRhSb and 17 for CeRhSn), the disorder introduced by both polycrystallinity and alloying must be screened out effectively by them. Parenthetically, one should note that CeRhSb has indeed an even number (18) of electrons, so the split hybridized-band structure provides the Kondo insulating state in this situation. On the contrary, the CeRhSn should then be metallic, as it contains odd number (17) of valence electrons. Note also that the whole discussion bases on the assumption that the $4f$ electrons of cerium are delocalized and contribute essentially to the band filling (otherwise, CeRhSn would be an insulator or a semimetal and CeRhSb should be a metal). This assumption is also not in disagreement with the almost integer valence of Ce, as determined from the XPS spectra. It is because the high-energy technique samples practically an instantaneous atomic configuration of Ce $4f$ electrons. This feature can be corroborated by noting that the lifetime of the $4f$ electrons on their parent atoms, when forming the heavy-fermion state, is $\tau_{\mathrm{HF}} = \hbar/(k_BT_K) \sim 10^{-12}$ s, whereas the photoemission is associated with the process on the time scale $\tau_v = \hbar/\Delta \sim 10^{-15}$ s, i.e., faster by 3–4 orders of magnitude. In essence, on the basis of results for the XPS technique one can talk about the mixed-valent configuration of cerium ($n_f < 1$), whereas on the basis of low-energy probes one should qualify this statement further by regarding the $4f$ electrons as heavy quasiparticles with an almost integer valence of Ce atoms. What is even more important, both ways of speaking are not in a mutual contradiction; they represent a complementary way of looking at the system, since in the GS analysis one deals with an atomic-state representation (describing $4f$ atomic states) and in the Anderson-lattice approach one describes the states very near the Fermi energy in the quasiparticle terms (i.e., in the momentum representation). Therefore, it is understandable that whereas the GS analysis provides a bare value of the hybridization (~ 0.15 eV), the value of T_K is provided by its renormalized counterpart [$V \to \tilde{V} = V(1-n_f)^{1/2} \sim V/10$]. This difference is universal feature of the HF systems and may result partly from the interpretation of the high-energy-probe data in terms of the Anderson impurity model, whereas in reality the $4f$ electrons form a periodic lattice.

The hybridization gap disappears with the increasing temperature.[45] The temperature diminution of the Kondo gap should be linear in T for temperature approaching the metallic state.[46] This theoretical prediction requires a further examination.

V. CONCLUSIONS

In this paper we have discussed a gradual disappearance of the Kondo gap for $CeRhSb_{1-x}Sn_x$, $x \leqslant 0.2$ and the evolution of the non-Fermi-liquid state for $x \geqslant 0.8$, i.e., we have observed a sequence of the states: Kondo insulator → heavy Fermi metal → non-Fermi liquid with the increasing x, which reflects the decrease of number of electrons by one per chemical formula when passing from CeRhSb to CeRhSn. It is clear that the random thermal motion will destroy this subtle quantum coherent state for temperature $T > T_K$. What is not yet clear from this work, is the setting of the NFL state

in the region $x \to 1$. It may be connected to the onset of the weak ferromagnetic state (Ref. 14). Namely, our preliminary specific-heat measurements show the presence of a small peak at $T \cong 6K$, providing the magnetic entropy change on the level of $0.02R\ln 2$. From this fact that the CeRhSn doped with Sb forms a weakly ferromagnetic Kondo-lattice state which is already absent for $x=0.9$, a presence of a quantum critical point near $x=0.9$ is possible, which drives the Sn-rich systems into a non-Fermi (non-Landau) metallic state. This is because the resistivity peak at $x=0.8$ of unknown origin appears already at $T \cong 7.8$ K.

In effect, in the single series of compounds, we observe almost all most interesting phenomena associated with the $4f$ intermetallic compounds containing strongly correlated electrons. Obviously, a detailed quantitative characterization of the $CeRhSb_{1-x}Sn_x$ systems should be reinforced by measurements carried out on high-quality single crystal samples.

One should note that in order to have both the Kondo insulating state for CeRhSb and a metallic state for CeRhSn we must assume that the Ce $4f$ electrons are itinerant. In this respect the Ce heavy-fermion and Kondo insulating compounds differ from the uranium compounds. This is because in the case of U systems the f-electron configuration is a mixture of $4f^2$ and $4f^3$ configurations. Therefore, due to the Hund's rule coupling,[47] we may then have a partition into localized and itinerant parts (i.e., a partial localization).[48] On the contrary, in the Ce compounds the $4f^1$ state delocalizes entirely, as the de Haas–van Alphen experiment show explicitly.[49] This last circumstance explains also a well-known fact that the Ce compounds have no obvious magnetic ordering, whereas many of the U compounds do order magnetically very often.

ACKNOWLEDGMENTS

Two of the authors (A.Ś. and T.Z.) acknowledge the support of the State Committee for Scientific Research (KBN), through Grant No. 2 P03B 098 25. One of the authors (J.S.) was supported by KBN, the Grant No. 2P03B 050 23; he also acknowledges the support of the Foundation for Science (FNP).

[1] T. Takabatake, F. Teshima, H. Fujii, S. Nishigori, T. Suzuki, T. Fujita, Y. Yamaguchi, J. Sakurai, and D. Jaccard, Phys. Rev. B **41**, 9607 (1990).
[2] S. K. Malik and D. T. Adroja, Phys. Rev. B **43**, 6277 (1991).
[3] T. Takabatake, G. Nakamoto, H. Tanaka, Y. Bando, H. Fujii, S. Nishigori, H. Goshima, T. Suzuki, T. Fujita, I. Oguro, T. Hiraoka, and S. K. Malik, Physica B **199-200**, 457 (1994); S. K. Malik, Latika Menon, V. K. Pecharsky, and K. A. Gschneidner, Jr., Phys. Rev. B **55**, 11 471 (1997)
[4] S. Doniach, Physica B **91**, 231 (1977).
[5] P. Coleman, Phys. Rev. Lett. **59**, 1026 (1987).
[6] P. A. Lee, T. M. Rice, J. W. Serene, L. J. Sham, and J. W. Wilkins, Comments Condens. Matter Phys. **XII**, 99 (1986); D. M. Newns and N. Read, Adv. Phys. **36**, 799 (1987).
[7] R. Doradziński and J. Spałek, Phys. Rev. B **56**, R14 239 (1997).
[8] T. J. Hammond, G. A. Gehring, M. B. Suvasini, and W. M. Temmerman, Phys. Rev. B **51**, 2994 (1995).
[9] J. Spałek and R. Doradziński, in *Magnetism and Electronic Correlations in Local-moment Systems: Rare Earth Elements and Compounds*, edited by M. Donath, P. A. Dowben, and W. Nolting (World Stientific, Singapore, 1998). p. 387; R.Doradziński and J. Spałek, Phys. Rev. B **58**, 3293 (1998).
[10] F. G. Aliev, V. V. Moshchalkov, M. K. Zalyalyutdinov, G. I. Pak, R. V. Scolozdra, P. A. Alekseev, V. N. Lazukov, and I. P. Sadikov, Physica B **163**, 358 (1990).
[11] T. Takabatake, Y. Nakazawa, M. Ishikawa, T. Sakakibara, K. Koga, and I. Oguro, J. Magn. Magn. Mater. **76&77**, 87 (1988).
[12] P. Schlottmann, Phys. Rev. B **54**, 12 324 (1996).
[13] L. Menon and S. Malik, Phys. Rev. B **52**, 35 (1995).
[14] A. Ślebarski, M. B. Maple, E. J. Freeman, C. Sirvent, M. Radłowska, A. Jezierski, E. Granado, Q. Huang, and J. W. Lynn, Philos. Mag. B **82**, 943 (2002).
[15] R. B. Griffiths, Phys. Rev. Lett. **23**, 17 (1969).
[16] A. H. Castro Neto, G. Castilla, and B. A. Jones, Phys. Rev. Lett. **81**, 3531 (1998).
[17] Y. Baer, G. Busch, and P. Cohn, Rev. Sci. Instrum. **46**, 466 (1975).
[18] O. K. Andersen and O. Jepsen, Phys. Rev. Lett. **53**, 2571 (1984); O. K. Andersen, O. Jepsen, and M. Sob, in *Electronic Structure and Its Applications*, edited by M. Yussouff (Springer, Berlin, 1987), p. 2.
[19] O. K. Andersen and O. Jepsen, Physica B **91**, 317 (1977).
[20] U. von Barth and L. Hedin, J. Phys. C **5**, 1629 (1972).
[21] C. D. Hu and D. C. Langreth, Phys. Scr. **32**, 391 (1985).
[22] K. Nakamura, Y. Kitaoka, K. Asayama, T. Takabatake, G. Nakamoto, H. Tanaka, and H. Fujii, Phys. Rev. B **53**, 6385 (1996).
[23] K. Izawa, T. Suzuki, T. Fujita, T. Takabatake, G. Nakamoto, H. Fujii, and K. Maezawa, Phys. Rev. B **59**, 2599 (1999).
[24] H. Kumigashira, T. Sato, T. Yokoya, T. Takahashi, S. Yoshii, and M. Kasaya, Physica B **281-282**, 284 (2000).
[25] A. Yanase and H. Harima, Prog. Theor. Phys. Suppl. **108**, 19 (1992).
[26] F. Ishii, Physica B **328**, 154 (2003).
[27] J. J. Yeh and I. Lindau, At. Data Nucl. Data Tables **32**, 1 (1985).
[28] S. Tougaard and P. Sigmund, Phys. Rev. B **25**, 4452 (1982).
[29] H. H. Hill, in *Plutonium 1970 and Other Actinides*, edided by W. N. Miner (AIME, 1970), Vol. 17, pp.1–19.
[30] T. Sato, H. Kadowaki, H. Yoshizawa, T. Takabatake, H. Fujii, and Y. Isikawa, J. Phys.: Condens. Matter **8**, 7127 (1996).
[31] O. Gunnarsson and K. Schönhammer, Phys. Rev. B **28**, 4315 (1983).
[32] J. C. Fuggle, F. U. Hillebrecht, Z. Zolnierek, R. Lässer, Ch. Freiburg, O. Gunnarsson, and K. Schönhammer, Phys. Rev. B **27**, 7330 (1983).
[33] P. W. Anderson, Phys. Rev. **124**, 41 (1961).
[34] S. Doniach and M. Šunjić, J. Phys. C **3**, 286 (1970).
[35] According to GS model, the coupling between the f^0 and f^1 configuration in the initial state ($N_f\Delta=2.1$ eV, where N_f is the de-

generacy of the f level) in relation to the energy separation between these states in the final state ($\sim$11 eV) is small, thus, the f^0 weight of the final state in the XPS spectrum is not much smaller than that in the initial state.

[36] E. Wuilloud, H. R. Moser, W.-D. Schneider, and Y. Baer, Phys. Rev. B **28**, 7354 (1983).

[37] C. Laubschat, E. Weschke, C. Holtz, M. Domke, O. Strebel, and G. Kaindl, Phys. Rev. Lett. **65**, 1639 (1990)

[38] E. Weschke, C. Laubschat, T. Simmons, M. Domke, O. Strebel, and G. Kaindl, Phys. Rev. B **44**, 8304 (1991).

[39] L. Z. Liu, W. Allen, O. Gunnarsson, N. E. Christensen, and O. K. Andersen, Phys. Rev. B **45**, 8934 (1992).

[40] A. J. Signorelli and R. G. Hayes, Phys. Rev. B **27**, 7330 (1983).

[41] Y. Baer, R. Hauger, Ch. Zürcher, M. Campagna, and G. W. Wertheim, Phys. Rev. B **18**, 4433 (1978).

[42] B. C. Sales and D. Wohlleben, Phys. Rev. Lett. **35**, 1240 (1975).

[43] A. S. Edelstein, J. Magn. Magn. Mater. **256**, 430 (2003).

[44] J. R. Schrieffer and P. A. Wolff, Phys. Rev. **149**, 491 (1966); J. Karbowski and J. Spałek (unpublished).

[45] T. Ekino, T. Takabatake, H. Tanaka, and H. Fujii, Physica B **206-207**, 837 (1995).

[46] J. Spałek and R. Doradziński, Acta Phys. Pol. A **96**, 677 (1999); **97**, 71 (2000).

[47] A. Klejnberg and J. Spałek, Phys. Rev. B **57**, 12 041 (1998).

[48] P. Fulde and G. Zwicknagl (private communication); G. Zwicknagl, A. N. Yaresko, and P. Fulde, Phys. Rev. B **65**, 081103(R) (2002); E. Runge, P. Fulde, D. V. Efremov, N. Hasselmann, and G. Zwicknagl, *ibid.* **69**, 155110 (2004).

[49] Y. Ōnuki, R. Settai, S. Araki, M. Nakashima, H. Ohkuni, H. Shishido, A. Thamizhavel, Y. Inada, Y. Haga, E. Yamamoto, and T. C. Kobayashi, Acta Phys. Pol. B **34**, 667 (2003), and references therein.